# Entanglement and thermalization in the extended Bose–Hubbard model after a quantum quench: A correlation analysis

Xiao-Qiang Su(苏晓强)[1,2,†], Zong-Ju Xu(许宗菊)[1,2], and You-Quan Zhao(赵有权)[1,2]

[1] *College of Physics and Information Engineering, Shanxi Normal University, Taiyuan* 030031, *China*
[2] *Key Laboratory of Spectral Measurement and Analysis of Shanxi Province, Shanxi Normal University, Taiyuan* 030031, *China*

(Received 14 April 2022; revised manuscript received 21 May 2022; accepted manuscript online 8 June 2022)

Exploring the role of entanglement in quantum nonequilibrium dynamics is important to understand the mechanism of thermalization in an isolated system. We study the relaxation dynamics in a one-dimensional extended Bose–Hubbard model after a global interaction quench by considering several observables: the local Boson numbers, the nonlocal entanglement entropy, and the momentum distribution functions. We calculate the thermalization fidelity for different quench parameters and different sizes of subsystems, and the results show that the degree of thermalization is affected by the distance from the integrable point and the size of the subsystem. We employ the Pearson coefficient as the measurement of the correlation between the entanglement entropy and thermalization fidelity, and a strong correlation is demonstrated for the quenched system.

**Keywords:** quantum quench, quantum entanglement, thermalization, extended Bose–Hubbard model

**PACS:** 05.70.Ln, 03.75.Lm, 03.65.Ud **DOI:** 10.1088/1674-1056/ac76b1

## 1. Introduction

The recent developments achieved in trapped ultracold atom gas experiments[1,2] have rapidly opened possibilities to explore many body physics in a highly controllable way. They have boosted a theoretical interest in the thermalization of the isolated quantum systems out of equilibrium. Quantum quench,[3–14] which is achieved by suddenly changing the parameters of the quantum systems, provides a natural platform to study these nonequilibrium dynamics. In the quench process, the system is prepared in an initial state $\rho_0$, which is mostly the ground state of the initial Hamiltonian $H_0$. Then, the model parameters are quickly changed and the quantum system undergoes a unitary time evolution with the new Hamiltonian $H$. After such a quench, the integrable system relaxes to a nonthermal steady state which can be described by the generalized Gibbs ensemble (GGE),[15–18] and the nonintegrable system thermalizes directly. Since thermalization is closely related to the integrability, it is interesting to know how thermalization is affected by the distance of the quenched system from the integrable point. We address this issue by changing the quench parameters away from the integrable point and examining the degree of thermalization.

The thermalization can be explained by the eigenstate thermalization hypothesis (ETH),[19–30] which states that the diagonal matrix elements of the observables are smooth functions of energy, and the off-diagonal elements are exponentially small in the system size. The ETH has been verified in a variety of models of spinless fermions,[22] hard-core[22–26] and soft-core Bosons,[27] spin ladder,[28] and spin chains.[29] The results for some local[25–29] and global[22–24,26] observables have been reported, and the entanglement was also discussed[25] for a two-dimensional hard-core Bose–Hubbard model with a perturbation theory truncated to second order.

A typical feature of the dynamics of the quenched system is the rapid linear growth of entanglement entropy to a stationary value which satisfies the volume law,[31–34] a detailed discussion can be found in the review paper.[33] This feature can be interpreted by the propagation of entangled quasiparticle.[31] The entanglement spectrum of the stationary state is recommended[35] as a criterion to distinguish the thermal state from the integrable[35] and localized states.[36,37] The increasing entanglement entropy is directly measured[38] in a Bose–Einstein condensate of $^{87}$Rb atoms loaded in a two-dimensional optical lattice. It is demonstrated that entanglement is related to thermalization in the scrambling process[34,39,40] and can be considered as the thermal entropy. Despite this progress, quantitative research on the correlation between entanglement and thermalization is still lacking. We therefore calculate this correlation in the relaxation dynamics of the quenched system by introducing the Pearson correlation coefficient (PCC) as a measurement.

The presentation is organized as follows: In Section 2, we introduce the model and quench proposal. The statistical ensembles used in this work are introduced in Section 3. In Section 4 we comparatively study the validity of the ETH by considering three different types of observables: the Boson number localized at some sites, the nonlocal entanglement between two subsystems and the global momentum distribution functions defined on the whole system. In Section 5,

†Corresponding author. E-mail: suxq@mail.ustc.edu.cn

© 2023 Chinese Physical Society and IOP Publishing Ltd 

the temporal dynamics of these observables and thermalization fidelity are obtained for different quench parameters. In Section 6, we calculate the correlation coefficients between entanglement entropy and thermalization fidelity for the time evolutions of the quenched system, and a strong correlation is demonstrated. A conclusion and discussion of our results are presented in Section 7.

## 2. Model and proposal

The realization of nonequilibrium dynamics can be conveniently achieved with cold atoms loaded in optical lattices.[9] By considering the nearest-neighbor interaction, the extended Bose–Hubbard model (EBHM)[41–45] is intriguing for the possible existence of the supersolid phase,[42,43,46,47] which was firstly observed in helium-IV.[48] Its Hamiltonian is

$$\hat{H} = -J\sum_{\langle i,j\rangle}(\hat{b}_i^{\dagger}\hat{b}_j + \text{H.c.}) + \frac{U}{2}\sum_i \hat{n}_i(\hat{n}_i - 1) + V\sum_{\langle i,j\rangle}\hat{n}_i\hat{n}_j, \quad (1)$$

where $\hat{b}_i^{\dagger}$ ($\hat{b}_i$) is the Boson creation (annihilation) operator and $\hat{n}_i = \hat{b}_i^{\dagger}\hat{b}_i$ is the local Boson number operator at site $i$, bracket $\langle i,j\rangle$ indicates that $i$ and $j$ are the nearest-neighbor sites. $J$ is the hopping parameter, $U$ is the on-site interaction and we set $U = 1$ here as the energy scaling, $V$ denotes the nearest-neighbor interaction. In the strong coupling region $J \to 0$, there are two insulator phases in EBHM, the Mott insulator phase (MI) and the mass-density-wave insulator phase (MDW). As $J$ increases, a quantum phase transition[41,49–52] to the superfluid phase occurs for both insulator phases. The quantum quench in a hard-core extended Bose–Hubbard model (HC-EBHM) was investigated in Refs. [22,23]. The HC-EBHM is integrable for one-dimensional lattice in the presence of only nearest-neighbor terms, thus the next-nearest-neighbor hopping and interaction are added to break the integrability.[22] The ETH and thermalization of the mean-field Shannon entropy, the momentum distribution functions, and the density–density correlation structure factors are discussed for integrable and nonintegrable quench parameters. The ETH of the off-diagonal elements is also discussed[5] for a one-dimensional HC-EBHM whose integrability is controlled by a power-law-decaying interaction.

We propose the nonequilibrium process via the paradigmatic setting of quantum quench in a one-dimensional EBHM with $N = 5$ Bosons filled in a lattice with $L = 9$ sites under the open boundary condition. We assume that the system is prepared in a mass-density-wave insulator phase ground state of an initial Hamiltonian with $J_0 = 0$ and $V_0 = 0.2$, which is a product state of each sites. Then at time $t = 0$, it is suddenly quenched to a final $J$ and keeps $V = 0.2$. The relaxation dynamics are obtained by considering the unitary time evolution under the new Hamiltonian. The EBHM is integrable for $J = 0$, and tends to be nonintegrable as $J$ increases. By controlling the final hopping parameters $J$ move away from the integrable point, we investigate the different thermalization features related to the integrability.

## 3. The statistic ensembles

### 3.1. Diagonal ensemble

Due to the recurrence theorem, a finite closed system returns arbitrarily close to its initial state on account of the entirely unitary evolution and never truly equilibrates.[53,54] However, we can focus on the transient nonequilibrium dynamics and define the equilibration in the sense of the time average as follows:

$$\rho_{\text{D}} = \lim_{T\to\infty}\frac{1}{T}\int_0^T \mathrm{e}^{-\mathrm{i}Ht}\rho_0\,\mathrm{e}^{\mathrm{i}Ht}\,\mathrm{d}t. \quad (2)$$

For the Hamiltonian with nondegenerate energy eigenvalues and nondegenerate energy level differences, $\rho_{\text{D}}$ is also called the diagonal ensemble.[55]

### 3.2. Microcanonical ensemble

Thermalization is considered[56–58] to take place when the diagonal ensemble gives the same predictions with the microcanonical ensemble for any local operator $\hat{A}$, as

$$\text{Tr}(\rho_{\text{D}}\hat{A}) = \text{Tr}(\rho_{\text{mic}}\hat{A}), \quad (3)$$

where the microcanonical ensemble can be defined as

$$\rho_{\text{mic}} = \frac{1}{N_{E_0,\Delta E}}\sum_{|E_\alpha - E_0|<\frac{\Delta E}{2}}|\alpha\rangle\langle\alpha|, \quad (4)$$

where $E_0$ is the mean energy of the quenched system, $\Delta E$ is the width of the energy window centered at $E_0$, and $N_{E_0,\Delta E}$ is the number of the energy eigenstates in the window.

### 3.3. Canonical ensemble

Another important thermal ensemble is the canonical ensemble as

$$\rho_T(E_n) = \frac{1}{Z}\exp\left(-\frac{E_n}{T}\right), \quad (5)$$

where $Z = \sum_n \exp(-\frac{E_n}{T})$ is the partition function, and we set the Boltzman constant $k = 1$ for simplify. It will be convenient to define the effective Gibbs temperature $T$ by employing

$$\sum_n E_n\rho_{\text{T}}(E_n) = \langle\psi_0|\hat{H}|\psi_0\rangle. \quad (6)$$

## 4. Eigenstate thermalization hypothesis

Let us firstly study the static statistics of the energy eigenstates for the quenched system. We numerically diagonalize the final Hamiltonian and calculate $\langle\hat{n}_i\rangle_\alpha = \langle\alpha|\hat{n}_i|\alpha\rangle$, which is the expectation value of the local Boson number $\hat{n}_i$ at site $i$ under the energy eigenstate $|\alpha\rangle$ with the eigenenergy $E_\alpha$. The

results are plotted as a function of $E_\alpha$ in the upper panels of Fig. 1. We choose two different final hopping parameters for comparison, $J = 0.1$, which is close to the integrable point, and $J = 1.6$ in the nonintegrable region. We find that the convergence to the ETH is affected by the integrability. For the weak hopping with $J = 0.1$ (circular dots), the profile gives a thick cloud of points rather than a smooth curve as in the situation with the strong hopping $J = 1.6$ (squared dots).

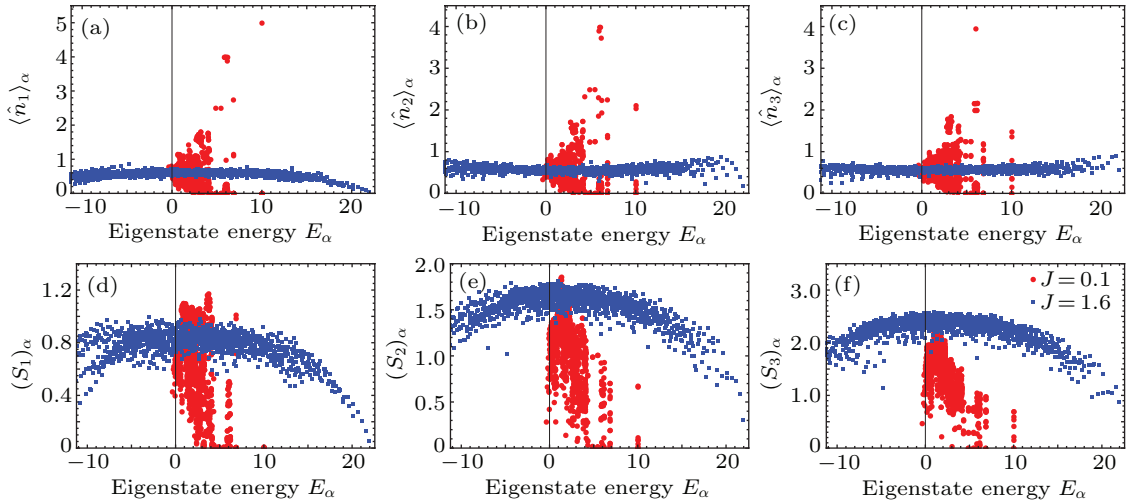



**Fig. 1.** Eigenstate thermalization hypothesis of the local Boson numbers and the entanglement entropy for the different hopping parameters $J = 0.1$ (circular points) and $J = 1.6$ (squared points). (a)–(c) The expectation values $\langle \hat{n}_i \rangle_\alpha$ of the local Boson number defined on site $i$ under the energy eigenstate $|\alpha\rangle$ as a function of the energy $E_\alpha$. (d)–(f) The entanglement entropy $(S_l)_\alpha$ between the $l$-site subsystem and its complement under the energy eigenstate $|\alpha\rangle$ as a function of the energy $E_\alpha$.

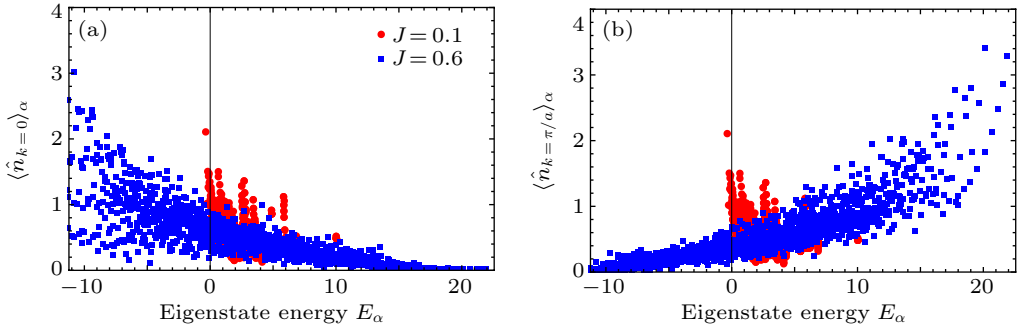



**Fig. 2.** Eigenstate thermalization hypothesis of the momentum distribution functions for the different hopping parameters $J = 0.1$ (circular points) and $J = 0.6$ (squared points). (a) The expectation values $\langle \hat{n}_{k=0} \rangle_\alpha$ of the momentum distribution function $\hat{n}_{k=0}$ under the energy eigenstate $|\alpha\rangle$ as a function of the energy $E_\alpha$. (b) The expectation values $\langle \hat{n}_{k=\pi/a} \rangle_\alpha$ of the momentum distribution function $\hat{n}_{k=\pi/a}$ under the energy eigenstate $|\alpha\rangle$ as a function of the energy $E_\alpha$.

It is interesting to verify the validity of the ETH for the nonlocal entanglement. We split the $L$-site lattice by subsystem $A$ with $l$ consecutive sites and the corresponding remainder $B$ with $L$–$l$ sites.[59,60] We use the second Rényi entropy of the reduced density matrix $\rho_A$ as the entanglement entropy, which can be defined as

$$S_A = -\log(\mathrm{Tr}\rho_A^2). \tag{7}$$

We calculate the entanglement entropy $(S_l)_\alpha$ between the subsystem and its complement under the eigenstates $|\alpha\rangle$. The features that similar to the results of the local Boson numbers can be observed in the lower panels of Fig. 1. The consistency with the ETH for the nonintegrable hopping parameter should lead to the thermalization of entanglement, as we will discuss in the next section.

The momentum distributions are global observables that can be measured conveniently in the cold atoms experiment. The operator of the quasimomentum distribution function $\hat{n}_k$ can be defined as

$$\hat{n}_k = \frac{1}{L}\sum_{i,j} \mathrm{e}^{-\mathrm{i}k(i-j)a}\hat{b}_i^\dagger \hat{b}_j, \tag{8}$$

where $a$ is the lattice constant. The expectation values $\langle \hat{n}_k \rangle_\alpha$ of the momentum distribution functions for $k = 0$ and $k = \pi/a$ under the eigenstates $|\alpha\rangle$ are calculated, and the results are plotted in Fig. 2. The thick horn-type distributions indicate the deviation from the standard ETH.

## 5. Thermalization

Thermalization of the quenched system can be described by the agreement of the expectation values of the local observables with the microcanonical ensemble. We thus directly

check the reduced density matrix of the subsystem and calculate the fidelity with the microcanonical ensemble, which is obtained as follows:

$$F_l = \mathrm{Tr}\left[\sqrt{\rho_l^{\frac{1}{2}}\rho_l^{\mathrm{mic}}\rho_l^{\frac{1}{2}}}\right], \tag{9}$$

where $\rho_l$ and $\rho_l^{\mathrm{mic}}$ are the reduced density matrix of the quenched system and the microcanonical ensemble, respectively. By beginning with an ordered initial state, the system undergoes local information scrambling to the nonlocal degree of freedom in the relaxation process. The fidelity initially increases rapidly and then saturates to 1 with weak fluctuations, as shown in Fig. 3(a). We further calculate the time-averaged fidelity $\bar{F}_l$ as a measurement of the degree of thermalization of the quenched system. The results for the different sizes of subsystem $l$ and the different final hopping parameters $J$ are plotted in Fig. 3(b). We find that the time-averaged fidelity increases with increasing $J$, indicating that thermalization is deeply related to the integrability of the quenched system which depends on the hopping parameter. The kinematic analysis by Popescu[56] based on Levy's lemma[61] has shown that the deviation from the microcanonical state is characterized by the ratio between the system size and the effective size of the environment. It can also be demonstrated that the time-averaged fidelity increases with decreasing subsystem size.

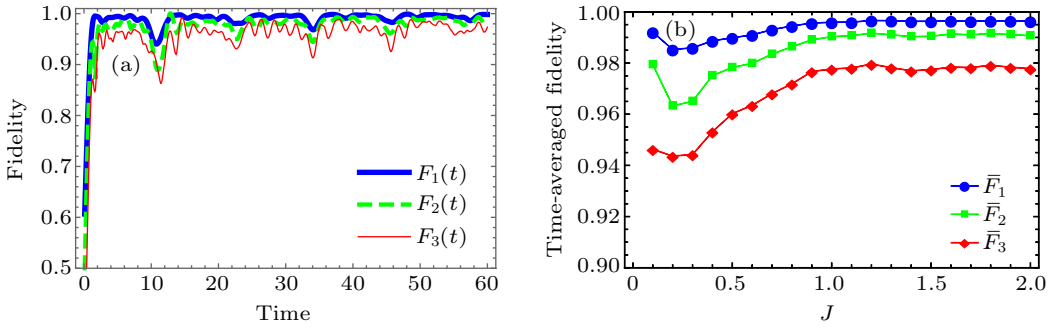



**Fig. 3.** The fidelity of the reduced density matrix of the subsystem with the microcanonical ensemble. (a) The time evolutions of the fidelity $F_l$ for the subsystems with the site numbers $l = 1$ (thick line), $l = 2$ (dashed line) and $l = 3$ (thin line), the final hopping parameter $J = 1.6$. (b) The time-averaged fidelity $\bar{F}_l$ within a period of evolution time $T = 1000$ for different final hopping parameters $J$.

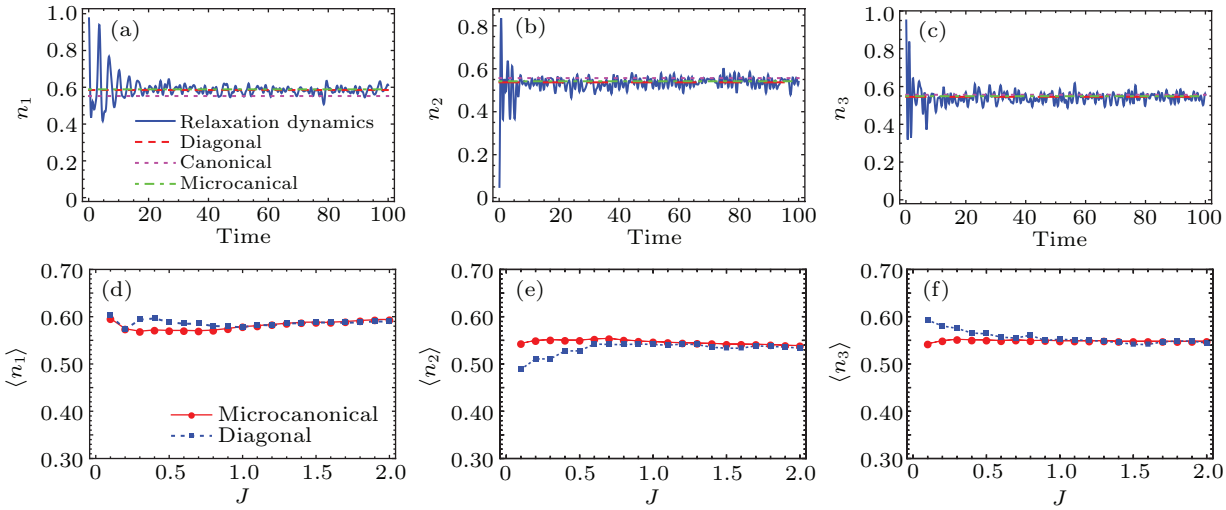



**Fig. 4.** (a)–(c) The time evolutions of the expectation values of the local Boson numbers $n_i$ (solid line) and the corresponding diagonal (dashed), canonical(dotted), and microcanonical (dashdotted) ensembles for comparison, the final hopping parameter $J = 1.6$. (d)–(f) The time-averaged (squared) and the microcanonical ensemble averaged (dotted) local Boson numbers versus final hopping parameters $J$, the total evolution time $T = 1000$.

Let us now continue the characterization of the thermalization by focusing on the temporal evolutions of the observables. Schematic curves for the expectation values of the local Boson numbers $n_i(t) = \langle\psi(t)|\hat{n}_i|\psi(t)\rangle$ are plotted in the upper panels of Fig. 4. We find that after a transient undulation, $n_i$ tends to the microcanonical ensemble and fluctuates around it. Thermalization is thus demonstrated by the agreement of the asymptotic values with the microcanonical ensemble. The time-averaged (diagonal ensemble) and the microcanonical ensemble averaged local Boson numbers $\langle n_i\rangle$ for different final hopping parameters $J$ are also plotted in the lower panels of Fig. 4. The divergence between the two ensembles tends to vanish as $J$ increases, with the system moving away from the integrable point.

Similar results are obtained for the time evolutions of the entanglement entropy. As we can see in Fig. 5, the entan-

glement entropy increases sharply from the initial zero and reaches a saturation value with fluctuations. The volume law of the saturated entanglement entropy is verified by the increases which is proportional to the sizes of the subsystems as $\langle S_l\rangle_{t\to\infty} \propto l$. The time-averaged (diagonal ensemble) and the microcanonical ensemble averaged entanglement entropy $\langle S_l\rangle$ are also plotted in the lower panels of Fig. 5. We find that, as the hopping parameters $J$ increases, the divergence to the microcanonical ensemble vanishes in a similar way as the local Boson numbers.

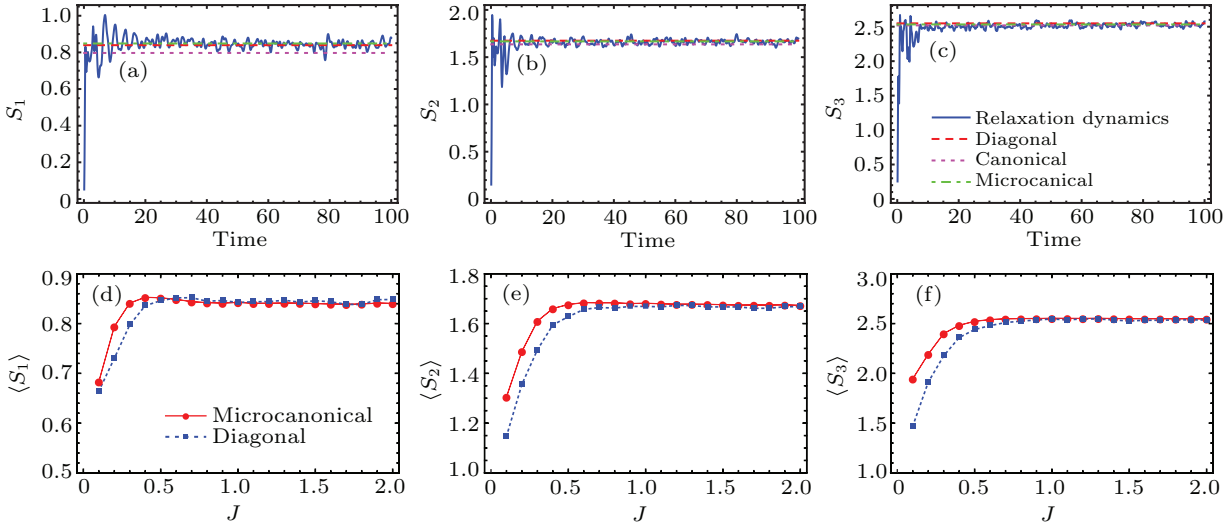



**Fig. 5.** (a)–(c) The time evolutions of the entanglement entropy $S_l$ and the corresponding diagonal (dashed), canonical (dotted), and microcanonical (dashdotted) ensembles for comparison, the final hopping parameter $J = 1.6$. (d)–(f) The time-averaged (squared) and the microcanonical ensemble averaged (dotted) entanglement entropy versus final hopping parameters $J$, the total evolution time $T = 1000$.

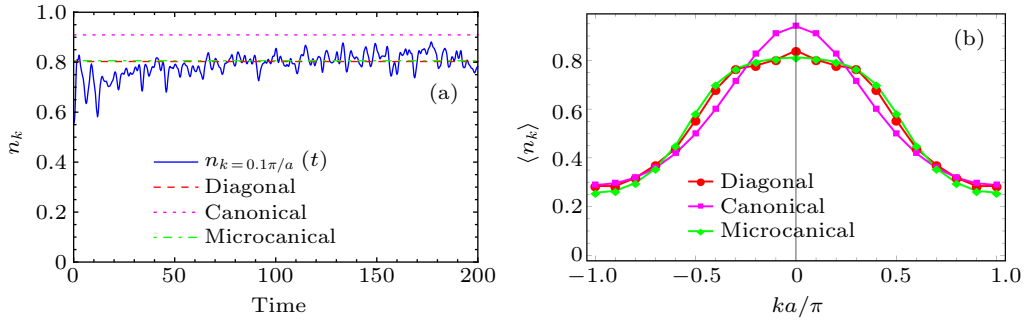



**Fig. 6.** (a) The time evolution of $n_k = 0.1\pi/a$ and the corresponding diagonal (dashed), canonical (dotted), and microcanonical (dashdotted) ensembles for comparison, the final hopping parameter $J = 0.6$. (b) The time-averaged (dotted), the canonical (squared) and microcanonical ensemble averaged (diamonded) momentum distribution functions $\langle n_k\rangle$ versus $k$, the final hopping parameter $J = 0.6$ and the total evolution time $T = 1000$.

We also calculate the time evolutions of the expectation values of the momentum distribution functions $n_k(t) = \langle\psi(t)|\hat{n}_k|\psi(t)\rangle$. A schematic curve for a chosen $k = 0.1\pi/a$ is plotted in Fig. 6(a). The time-averaged (diagonal ensemble), canonical and microcanonical ensemble averaged momentum distribution functions $\langle n_k\rangle$ versus $k$ are also plotted in Fig. 6(b). We find that the time-averaged momentum distribution functions are roughly consistent with the microcanonical ensemble, and their divergences are mainly at the central $k = 0$ and at the endpoints $k = \pm\pi/a$. Of course, their divergences may appear at other $k$ for conservation (on account of the normalization of the distribution function). These divergences can be discerned from the dispersed points in the ETH pictures of Fig. 2. It is worth mentioning that, as a global observable, the fluctuation amplitude of $n_k$ does not decay quickly with the information scrambling process as the two observables mentioned above, even though the time-averaged diagonal ensemble agrees with the microcanonical ensemble finally (as shown in Fig. 6).

## 6. Thermalization versus entanglement

As the most important resource in quantum information processing, quantum entanglement also plays a central role in the thermalization of the isolated quantum system. It is well known that statistical mechanics relies on the maximization of entropy for a system at thermal equilibrium. However, an isolated quantum system undergoing entirely unitary evolution can be described by a pure quantum state with zero entropy. However, when we consider the quantum entanglement, the subsystems interacting with each other become entangled and

local entropy can be created. As a result, the quantum states of the subsystems are decohered to mixed states, allowing the local observables of the subsystem to be described by the statistical physics. Therefore, studying on the correlation between entanglement and thermalization will help us to understand the physical mechanism of thermalization in an isolated system.

We schematically plot the entanglement evolution curve together with the thermalization fidelity in Fig. 7. We can find that there are obvious synchronous fluctuations for the early stage revivals in the relaxation dynamics. To describe this correlation, we introduce the Pearson correlation coefficient (PCC) of two variables, which is defined as

$$r(A,B) = \frac{\mathrm{Cov}(A,B)}{\sigma_A \sigma_B}, \tag{10}$$

where the covariance

$$\mathrm{Cov}(A,B) = \frac{1}{T}\int_0^T A(t)B(t)\,\mathrm{d}t - \overline{A}\cdot\overline{B}, \tag{11}$$

and the deviation $\sigma_A$ satisfies

$$\sigma_A^2 = \frac{1}{T}\int_0^T A(t)^2\,\mathrm{d}t - \overline{A}^2, \tag{12}$$

where $\overline{A}$ denotes the temporal average of variable $A$,

$$\overline{A} = \frac{1}{T}\int_0^T A(t)\,\mathrm{d}t. \tag{13}$$

The PCC is a number between $-1$ and $+1$, which indicates that two variables are linearly related. A correlation $r = 1$ ($r = -1$) means that the two variables are perfectly positively (negatively) related, and $r = 0$ means that the two variables do not have any linear correlation.

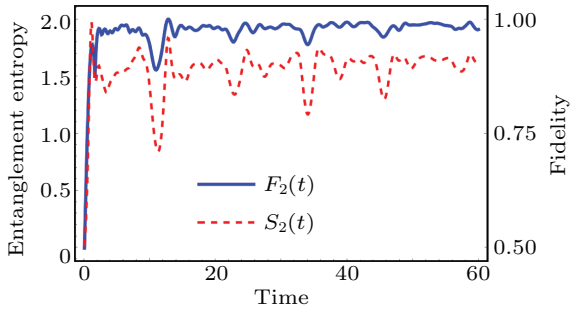



**Fig. 7.** Schematic comparison of the time evolutions of the entanglement entropy $S_2$ and the thermalization fidelity $F_2$, for the final hopping parameter $J = 1.6$.

The PCC between the entanglement entropy and the thermalization fidelity are obtained within a period of evolution time $T = 1000$ after the quench. The results for the different final hopping parameters $J$ and the different sizes of subsystem $l$ are plotted in Fig. 8. We find that all the values of the PCC are close to or above 0.8, indicating a strong correlation between entanglement and thermalization.

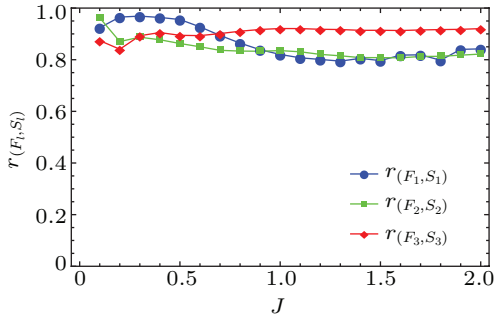



**Fig. 8.** The Pearson correlation coefficients $r_{(F_l,S_l)}$ between the entanglement entropy $S_l$ and the thermalization fidelity $F_l$ for different final hopping parameters $J$, the total evolution time $T = 1000$.

The correlation between entanglement and thermalization can be explained as follows. The initial state of the quenched system is a product state with zero local entropy, and the asymptotic equilibrium state becomes entangled. The fidelity of the reduced density matrix increases as the quantum state of the subsystem tends to the microcanonical ensemble after the quench, the entanglement which can be denoted by the local entropy increases correspondingly. It results in the synchronous fluctuations of the entanglement entropy and the thermalization fidelity.

## 7. Discussion and conclusion

We have studied the relaxation dynamics in a one-dimensional extended Bose–Hubbard model after the global quench of the hopping parameter $J$. The eigenstate thermalization hypotheses are discussed by considering the expectation values of three observables: the local Boson numbers, the entanglement entropy and the momentum distribution functions. The temporal evolutions of these observables are also obtained, and the time-averaged diagonal ensembles are consistent with the microcanonical ensembles for the local Boson numbers, the entanglement entropy and roughly for most of the momentum distribution functions. The fidelity of the reduced density matrix of the subsystem with the microcanonical ensemble is calculated for the different final hopping parameters, and the results show that the degree of thermalization is affected by the distance from the integrable point and the size of the subsystem. A strong correlation between entanglement and thermalization is also verified by introducing the Pearson correlation coefficient of the entanglement entropy and the thermalization fidelity, indicating that entanglement with the environment is very important in the thermalization process.

The correlation between entanglement and thermalization is complicated. The PCC is a measurement that only accounts for the linear correlation, and the values are also related to the chosen measurements of entanglement and degree of thermalization. It is hopeful that this work stimulates further research on this correlation.

## Acknowledgements

Project supported by the National Natural Science Foundation of China (Grant No. 11147110), and the Natural Science Youth Foundation of Shanxi Province, China (Grant No. 2011021003).

## References

[1] Kinoshita T, Wenger T and Weiss D S 2006 *Nature* **440** 900
[2] Tang Y, Kao W, Li K Y, Seo S, Mallayya K, Rigol M, Gopalakrishnan S and Lev B L 2018 *Phys. Rev. X* **8** 021030
[3] Greiner M, Mandel O, Hänsch T W and Bloch I 2002 *Nature* **419** 51
[4] Rigol M 2009 *Phys. Rev. A* **80** 053607
[5] Khatami E, Pupillo G, Srednicki M and Rigol M 2013 *Phys. Rev. Lett.* **111** 050403
[6] Sorg S, Vidmar L, Pollet L and Heidrich-Meisner F 2014 *Phys. Rev. A* **90** 033606
[7] Gogolin C, Mueller M P and Eisert J 2011 *Phys. Rev. Lett.* **106** 040401
[8] Titum P, Iosue J T, Garrison J R, Gorshkov A V and Gong Z X 2019 *Phys. Rev. Lett.* **123** 115701
[9] Chen Z, Tang T, Austin J, Shaw Z, Zhao L and Liu Y 2019 *Phys. Rev. Lett.* **123** 113002
[10] Titum P and Maghrebi M F 2020 *Phys. Rev. Lett.* **125** 040602
[11] Gong Z and Ueda M 2018 *Phys. Rev. Lett.* **121** 250601
[12] Guardado-Sanchez E, Brown P T, Mitra D, Devakul T, Huse D A, Schauss P and Bakr W S 2018 *Phys. Rev. X* **8** 021069
[13] Ge Z Y, Huang R Z, Meng Z Y and Fan H 2022 *Chin. Phys. B* **31** 020304
[14] Su X Q and Zhao Y Q 2020 *Chin. Phys. B* **29** 120506
[15] Jaynes E T 1957 *Phys. Rev.* **106** 620
[16] Jaynes E T 1959 *Phys. Rev.* **108** 171
[17] Rigol M, Dunjko V, Yurovsky V and Olshanii M 2007 *Phys. Rev. Lett.* **98** 050405
[18] Murakami Y, Takayoshi S, Kaneko T, Sun Z, Gole D, Millis A J and Werner P 2022 *Commun. Phys.* **5** 23
[19] Srednicki M 1994 *Phys. Rev. E* **50** 888
[20] Srednicki M 1999 *J. Phys. A: Math. Gen.* **32** 1163
[21] Deutsch J M 1991 *Phys. Rev. A* **43** 2046
[22] Santos L F and Rigol M 2010 *Phys. Rev. E* **81** 036206
[23] Santos L F and Rigol M 2010 *Phys. Rev. E* **81** 031130
[24] Rigol M, Dunjko V and Olshanii M 2008 *Nature* **452** 854
[25] Khlebnikov S and Kruczenski M 2014 *Phys. Rev. E* **90** 050101(R)
[26] D'Alessio L, Kafri Y, Polkovnikov A and Rigol M 2016 *Adv. Phys.* **65** 239
[27] Biroli G, Kollath C and Läuchli A M 2010 *Phys. Rev. Lett.* **105** 250401
[28] Steinigeweg R, Khodja A, Niemeyer H, Gogolin C and Gemmer J 2014 *Phys. Rev. Lett.* **112** 130403
[29] Brenes M, LeBlond T, Goold J and Rigol M 2020 *Phys. Rev. Lett.* **125** 070605
[30] Sugimoto S, Hamazaki R and Ueda M 2021 *Phys. Rev. Lett.* **126** 120602
[31] Calabrese P and Cardy J 2005 *J. Stat. Mech.* **2005** P04010
[32] Alba V and Calabrese P 2017 *Proc. Natl. Acad. Sci. USA* **114** 7947
[33] Hu M L, Hu X, Wang J C, Peng Y, Zhang Y R and Fan H 2018 *Phys. Rep.* **762–764** 1
[34] Lewis-Swan R J, Safavi-Naini A, Bollinger J J and Rey A M 2019 *Nat. Commun.* **10** 1581
[35] Poilblanc D 2011 *Phys. Rev. B* **84** 045120
[36] Yang Z C, Hamma A, Giampaolo S M, Mucciolo E R and Chamon C 2017 *Phys. Rev. B* **96** 020408(R)
[37] Geraedts S D, Nandkishore R and Regnault N 2016 *Phys. Rev. B* **93** 174202
[38] Kaufman A M, Tai M E, Lukin A, Rispoli M and Greiner M 2016 *Science* **353** 794
[39] Sekino Y and Susskind L 2008 *J. High Energy Phys.* **2008(10)** 065
[40] Swingle B, Bentsen G, Schleier-Smith M and Hayden P 2016 *Phys. Rev. A* **94** 040302(R)
[41] Niyaz P, Scalettar R T, Fong C Y and Batrouni G G 1991 *Phys. Rev. B* **44** 7143
[42] Scarola V M and Das Sarma S 2005 *Phys. Rev. Lett.* **95** 033003
[43] Ng K K, Chen Y C and Tzeng Y C 2010 *J. Phys.: Condens. Matter* **22** 185601
[44] Wang Y C, Zhang W Z, Shao H and Guo W A 2013 *Chin. Phys. B* **22** 096702
[45] Su X Q and Wang A M 2012 *Chin. J. Phys.* **50** 500
[46] Diehl S, Baranov M, Dalay A J and Zoller P 2010 *Phys. Rev. Lett.* **104** 165301
[47] Li J R, Lee J, Huang W, Burchesky S, Shteynas B, Top F Çağri, Jamison A O and Ketterle W 2017 *Nature* **543** 91
[48] Kim E and Chan M H W 2004 *Nature* **427** 225
[49] Sengupta P, Pryadko L P, Alet F, Troyer M and Schmid G 2005 *Phys. Rev. Lett.* **94** 207202
[50] Pai R V and Pandit R 2005 *Phys. Rev. B* **71** 104508
[51] Kühner T D and Monien H 1998 *Phys. Rev. B* **58** R14741(R)
[52] Kühner T D, White S R and Monien H 2000 *Phys. Rev. B* **61** 12474
[53] Bocchieri P and Loinger A 1957 *Phys. Rev.* **107** 337
[54] Percival I C 1961 *J. Math. Phys.* **2** 235
[55] Cassidy A C, Clark C W and Rigol M 2011 *Phys. Rev. Lett.* **106** 140405
[56] Popescu S, Short A J and Winter A 2006 *Nature Physics* **2** 754
[57] Reimann P 2008 *Phys. Rev. Lett.* **101** 190403
[58] Riera A, Gogolin C and Eisert J 2012 *Phys. Rev. Lett.* **108** 080402
[59] D'Espagnat B 1984 *Phys. Rep.* **110** 201
[60] D'Espagnat B 1999 *Conceptual Foudations of Quantum Mechanics* (New York: Perseus Books)
[61] Linden N, Popescu S, Short A J and Winter A 2009 *Phys. Rev. E* **79** 061103